

Quantitative Evaluation of Quantum/Classical Neural Network Using a Game Solver Metric

SUZUKAZE KAMEI¹, HIDEAKI KAWAGUCHI², SHIN NISHIO¹, and Tatakahiko Satoh¹

¹Faculty of Science and Technology, Keio University, Yokohama, Kanagawa 223-8522 Japan

²Graduate School of Science and Technology, Keio University, Yokohama, Kanagawa 223-8522 Japan

Corresponding author: Suzukaze Kamei (e-mail: suzukaze_kamei@keio.jp).

SK, HK, SN, and TS are supported by JST Moonshot R&D Grant Number JPMJMS226C. SK and TS are also supported by JST COI-NEXT Grant Number JPMJPF2221. SN is also supported by JSPS KAKENHI Grant Number JP22KJ1436. TS is also supported by MEXT KAKENHI Grant Number 22K1978.

ABSTRACT To evaluate the performance of quantum computing systems relative to classical counterparts and explore the potential for quantum advantage, we propose a game-solving benchmark based on Elo ratings in the game of tic-tac-toe. We compare classical convolutional neural networks (CNNs), quantum convolutional neural networks (QCNNs), and hybrid classical-quantum models by assessing their performance against a random-move agent in automated matches. Additionally, we implement a QCNN integrated with quantum communication and evaluate its performance to quantify the overhead introduced by noisy quantum channels. Our results show that the classical-quantum hybrid model achieves Elo ratings comparable to those of classical CNNs, while the standalone QCNN underperforms under current hardware constraints. The communication overhead was found to be modest. These findings demonstrate the viability of using game-based benchmarks for evaluating quantum computing systems and suggest that quantum communication can be incorporated with limited impact on performance, providing a foundation for future hybrid quantum applications.

INDEX TERMS Quantum Machine Learning, Quantum Communication, Quantum/Classical Algorithm, Rating System, Tic-Tac-Toe Solver

I. INTRODUCTION

QUANTUM computers have brought new possibilities to many previously difficult problems for classical computers to solve [1], [2]. In recent years, the development of quantum computers has made remarkable progress. Noise Intermediate-Scale Quantum (NISQ) computers exceeding 1,000 qubits have emerged, and it is anticipated that early Fault-Tolerant Quantum Computers (FTQC) will also appear in the not-so-distant future [3]. With further advancements in both hardware and algorithms, the potential for applying quantum advantage to real-world problems is increasingly becoming a reality.

Current benchmarks for quantum computers, such as random circuit sampling, demonstrate quantum advantages in limited tasks [4]. However, evidence supporting their superiority in solving real-world problems remains inconclusive [5]. Furthermore, the absence of common and standardized metrics for computational performance presents a significant challenge in evaluating the potential societal and practical impact of future quantum computing technologies.

Classical game AIs, such as AlphaZero [6], have been

highly successful and have significantly outperformed human abilities in perfect-information zero-sum games. While quantum game AIs have been proposed for solving single-player puzzle games using search algorithms [7], algorithms that can adapt to dynamically changing board information in competitive games remain unexplored. By utilizing a unified metric, it becomes possible to compare the performance of quantum and classical systems directly.

In this research, we propose a novel approach for evaluating the performance of quantum and classical computers through competitive board games. An overview of the proposed game-solving framework—including client-side inference, quantum communication, and server-side processing—is illustrated in Fig. 1. Game-playing AI provides a suitable platform for comprehensive performance assessment, as it involves data structure manipulation, decision-making, and real-time optimization.

The objective of this study is to quantitatively assess the capabilities of quantum computers using competitive games. To this end, we adopt the following methodology:

- 1) Develop a game engine incorporating classical and

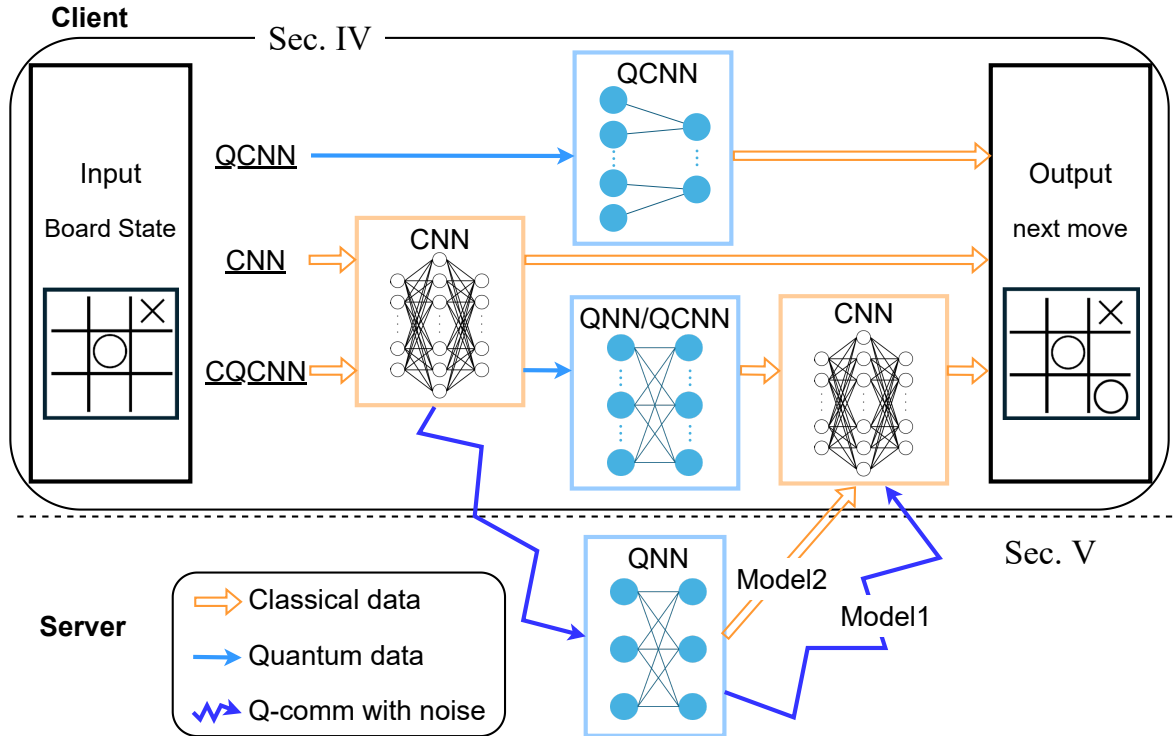


FIGURE 1. The game solver initially runs on the client, receiving the board state and selecting the next move using a classical, quantum, or hybrid neural network. In the Quantum Internet setup, a noisy quantum communication channel connects the client and server. The client processes the input with a classical neural network, encodes the output into qubits, and sends them through the quantum channel. The server then applies a quantum neural network and returns either classical measurement results or unmeasured qubits. The client uses the received data to determine the next move.

quantum neural networks.

- 2) Design four policy types—random, classical, quantum, and classical-quantum hybrid—and compare their performance.
- 3) Evaluate each engine using Elo ratings to provide a unified performance metric.

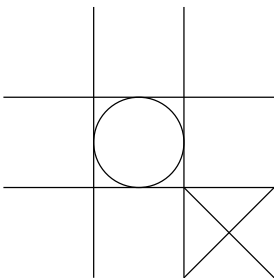


FIGURE 2. Tic-Tac-Toe game board consisting of 9 squares. 2 players place O and X alternately in the squares. The first player to place O or X in a vertical, horizontal, or diagonal line wins the game. If neither of them is aligned, the game ends in a tie.

While this game is extremely simple and cannot concretely clarify areas where quantum computers outperform classical methods, the design that can adapt to more complex games is important for this unexplored topic.

Furthermore, we evaluate the impact of connecting quantum devices with varying performance levels, in anticipation of future quantum communication applications. Just as classical high-performance computing is widely accessed via the cloud, similar usage scenarios are expected for quantum devices. In this study, we examine the practicality of quantum applications over the quantum Internet (QI) by analyzing the communication overhead caused by noise, assuming a client with limited quantum resources and a server with abundant ones. While the detailed QI protocols involving entanglement are beyond our scope, we construct and test simplified models under two scenarios, based on the client’s quantum resource availability.

To explore this approach, we first review the machine learning techniques and Elo rating system used in our study (Sec. II). We then describe the architecture of the proposed game engines (Sec. III) and evaluate their performance (Sec. IV). Next, we introduce the quantum Internet model and assess the performance of game engines operating within this setting (Sec. V). Finally, we conclude with a summary of our findings and discuss future research directions (Sec. VI).

II. PRELIMINARIES

A. REINFORCEMENT LEARNING

Reinforcement learning is a method of learning to make the optimal choice in a particular environment. Unlike supervised

and unsupervised learning, it aims to learn through the interaction between the environment and the agent and maximizing the reward so that the agent can cope with unknown domains.

For example, in the case of tic-tac-toe, the environment corresponds to the game board, and the agent is the game engine incorporating the neural network. Learning proceeds based on the board state, the reward received, and the next move determined by the engine (Fig. 3).

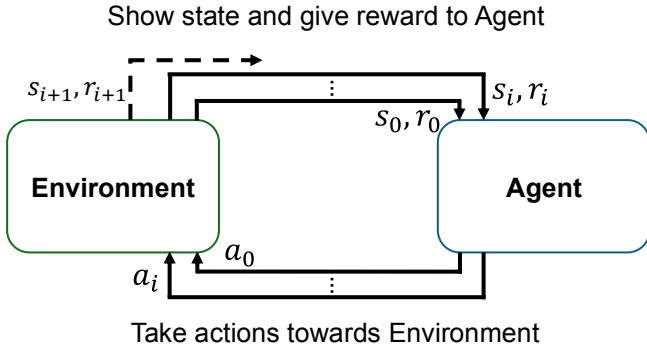


FIGURE 3. Schematic diagram of agent–environment interaction in reinforcement learning. At each time step i , the environment provides the current board state s_i and reward r_i to the agent. The agent then selects an action a_i based on this input. The environment updates the board accordingly and returns the next state s_{i+1} and reward r_{i+1} . This cycle is repeated throughout the game.

There is a strong connection between reinforcement learning and game AI, especially in games such as chess and shogi. Competitive games are well-suited for reinforcement learning because outcomes (win/loss) are clearly defined and player performance can be quantitatively evaluated. As reinforcement learning algorithms have evolved, game AI has improved in parallel.

Q-learning is one of the foundational algorithms in reinforcement learning. In this study, we developed and evaluated a game engine based on Q-learning. This section provides a brief overview of the algorithm [8].

Reinforcement learning aims to maximize the expected return from a given strategy. When the environment follows a Markov decision process, the expected value can be divided into two types: a *state-value function*, which estimates the value of a state, and an *action-value function*, which estimates the value of taking a specific action in a given state.

Q-learning enables efficient reinforcement learning by iteratively updating the action-value function. The update rule is defined as follows:

$$Q(s_i, a_i) \leftarrow Q(s_i, a_i) + \alpha \left[r_{i+1} + \gamma \max_{a_{i+1}} Q(s_{i+1}, a_{i+1}) - Q(s_i, a_i) \right] \quad (1)$$

Here, $Q(s_i, a_i)$ represents the estimated return of taking action a_i in state s_i . α is the learning rate, and γ is the discount factor, which determines the importance of future rewards. r_{i+1} is the reward received after performing action

a_i , and s_{i+1} is the resulting next state. The update adjusts the current estimate toward the target value, which consists of the immediate reward plus the discounted maximum future value.

B. QUANTUM MACHINE LEARNING

Quantum machine learning [9], [10] has emerged as a promising application of quantum computing. It aims to develop learning algorithms that leverage quantum properties to outperform classical machine learning in terms of computational efficiency and model expressiveness.

In particular, quantum neural networks (QNNs) have been proposed as quantum analogues of classical neural networks. When processing classical data, a typical QNN pipeline involves three stages: encoding the data into quantum states, processing it using parameterized quantum circuits (ansatz), and measuring the output to obtain classical values. These values are used to optimize parameters via classical computation.

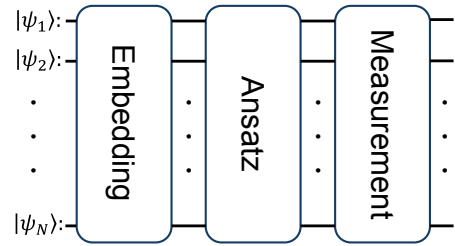


FIGURE 4. Structure of a quantum neural network (QNN). A typical QNN consists of three components: (1) *Embedding* – classical data is encoded into quantum states $|\psi_k\rangle$; (2) *Ansatz* – parameterized quantum circuits optimized via classical computation; and (3) *Measurement* – quantum states are measured to produce classical outputs.

Quantum Neural Network Architectures

Quantum machine learning offers a variety of neural network architectures, each designed to address different aspects of performance and scalability.

One such approach is the hybrid neural network (HNN), which combines classical and quantum components. For example, classical neural networks (CNNs) may be placed before or after a quantum layer, or quantum circuits may be used to perform certain computations such as gradient descent [11], [12]. These hybrid models aim to exploit the strengths of both paradigms, making them suitable for near-term quantum devices.

Another notable architecture is the quantum convolutional neural network (QCNN) [13], which is inspired by classical convolutional networks but designed to operate on quantum states. QCNNs can achieve more efficient learning with fewer parameters than general QNNs. Moreover, they have been shown to mitigate the *barren plateau* problem [14], in which gradients vanish during training, hindering effective optimization.

The QCNN ansatz consists of alternating convolution and pooling layers (Fig. 16). In the convolutional layers, entanglement between qubits is used to extract local features. The pooling layers reduce dimensionality by discarding a subset

of qubits, rather than aggregating information as in classical CNNs. Repeating these layers enables hierarchical feature extraction and supports scalable learning.

These architectures demonstrate how quantum machine learning can be structured to balance expressivity and trainability. Hybrid models are particularly promising in the current era of noisy intermediate-scale quantum (NISQ) devices, while QCNNS offer a scalable framework for leveraging quantum entanglement and feature abstraction in learning tasks.

C. ELO RATING

Elo rating [15]–[17] is a widely used system for quantifying the strength of individual players in competitive games, such as chess. It enables an approximate comparison of player skill levels, regardless of game order or the number of opponents.

In our setting, we define the Elo rating of player A as R_A and that of player B as R_B . When A and B compete, the probability that A wins is given by:

$$W_{AB} = \frac{1}{10^{(R_B - R_A)/400} + 1} \quad (2)$$

Using this probability, the rating of player A is updated as:

$$R'_A = R_A + K(N_{\text{wins}} - N_{\text{games}} \cdot W_{AB}), \quad (3)$$

where N_{wins} is the number of games A won, N_{games} is the total number of games played (excluding draws), and K is a scaling factor that controls the update sensitivity.

Figure 5 shows the relationship between the rating difference ($R_B - R_A$) and the expected winning probability W_{AB} , as defined in Eq. (2). From the curve, we observe that a rating difference of approximately 70 corresponds to a winning probability of about 60%.

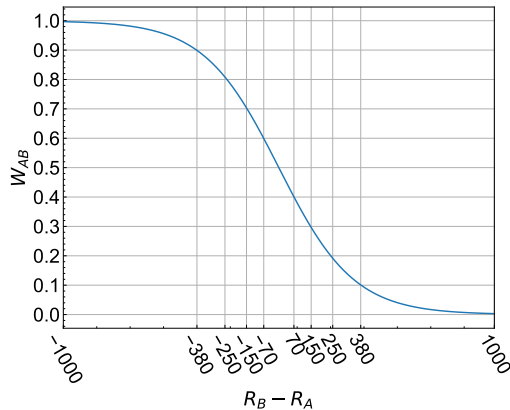


FIGURE 5. Relationship between rating difference and winning rate.

D. QUANTUM MACHINE LEARNING WITH CLIENT-SERVER MODEL

1) Overview of the Client-Server Model

Quantum computers require large-scale infrastructure, so they are typically owned by major vendors rather than individual

users. In this situation, the client sends some classical or quantum information to the server owned by the vendors, and then the vendor executes the costly part of the computation. This type of computational setup is referred to as the client-server model, and it is regarded as an application of the quantum Internet. The client-server model not only enables physically distributed computing systems but also offers a variety of additional advantages when quantum machine learning tasks use this model [18], [19]. One can consider a scenario where the client-server model is adopted in the following manner: the client encodes classical data into quantum states and sends them to the server; the server calculate ansatz to perform the necessary quantum operations; then, the resulting quantum states are returned to the client, who performs the measurements and processes the outcomes.

2) Advantages of the Model

One of the most significant benefits of this model is data privacy. Since the raw classical data remains on the client side and is embedded into quantum states locally, the server, which may be untrusted or a third-party quantum cloud provider, never gains access to the original data. This structure allows secure delegation of quantum resources while ensuring that sensitive input information remains protected.

Another advantage is greater flexibility in classical optimization. The client retains full responsibility for processing measurement results, computing loss functions, and updating parameters during optimization. This separation allows integration with a wide range of classical optimization algorithms without needing to expose internal training dynamics to the server. Additionally, because the quantum server performs only the ansatz operations, this model helps reduce quantum circuit depth, which is particularly important when working with near-term quantum devices (NISQ era) that suffer from decoherence and gate errors.

3) Roles and Use Cases

Moreover, this model supports a clear separation of roles between data owners and model providers. The client may represent an entity with proprietary data, while the server hosts a proprietary model or provides quantum computing resources. This separation encourages secure collaboration and scalability. Importantly, the model also opens doors to federated or blind quantum learning, where multiple clients can train using local data and shared quantum resources without exposing their private information to each other or the server.

4) Implications for Noisy Quantum Communication

Finally, having the client perform measurements locally can lead to greater control over noise and readout errors, avoiding server-side biases or inaccuracies in quantum measurement. Together, these benefits make this client-server model a promising candidate for secure, efficient, and scalable quantum machine learning in real-world applications.

III. TIC-TAC-TOE ENGINES

In this section, we describe three types of game engines, each utilizing a classical, quantum, or hybrid neural network architecture. All neural networks are trained using classical optimization methods. Quantum circuits are integrated into the PyTorch framework via the `TorchConnector` provided by Qiskit [20]. We employ Huber Loss [21] as the loss function and the Adam optimizer [22] for weight updates.

The overall structure of the neural network-based engines is illustrated in Fig. 6. Since neural networks require numerical input and output, the tic-tac-toe board is encoded as a 9-element vector, where O is represented as +1, X as -1, and empty squares as 0. The network outputs a vector of nine values, each corresponding to a board cell, and the cell with the highest value is chosen as the next move.

We adopt a simple reinforcement learning scheme by replacing the conventional Q-table with a neural network model. The Q-learning update rule, described in Eq. (1), is applied after each game, with rewards of +1 for a win, -1 for a loss, and 0 for a draw.

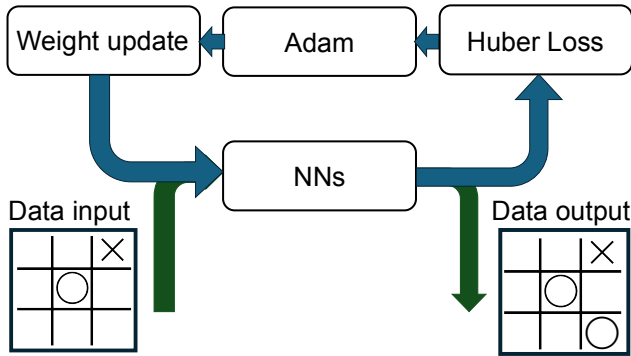


FIGURE 6. Scheme of neural network-based engines. NNs such as QNN (Fig. 4), CNN, and QCNN are integrated into the engine. The input game board is encoded into numerical values and passed through the network to generate an output vector. The engine selects the next move based on the cell with the highest output value. Training is performed using Huber Loss and the Adam optimizer to update network weights.

A. CLASSICAL NEURAL NETWORKS (CNN, CCNN)

The engine is constructed by combining CNNs and CCNNs (Fig. 7). The engine using CCNNs was structured to perform convolution on the input board, and then to obtain output using CNNs. Two variants, referred to as "Stronger" and "Weaker," differ in the number of layers and parameters. The architectures are summarized in Table 1.

B. QUANTUM CONVOLUTIONAL NEURAL NETWORKS (QCNN)

The QCNN-based engines differ in their choice of embedding circuits (HEE, TPE, ZFeatureMap, ZZFeatureMap). All models use 18 qubits, with the 9-cell input duplicated to match the quantum register size. Details of the quantum circuit designs are provided in Appendix A-A.

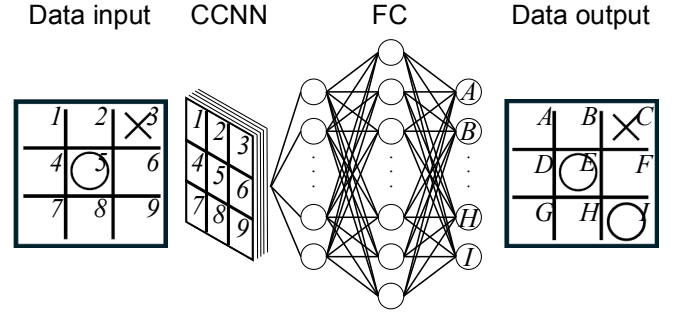


FIGURE 7. Data flow in the classical convolutional neural network (CCNN) engine. The tic-tac-toe board is encoded into numerical values and passed through convolutional layers, followed by fully connected layers. The output consists of nine values corresponding to the board cells, and the move with the highest score is selected.

The number of shots in the measurement is set to 1000, and half of each qubit is measured in the Z basis, and the expected value is taken as the output.

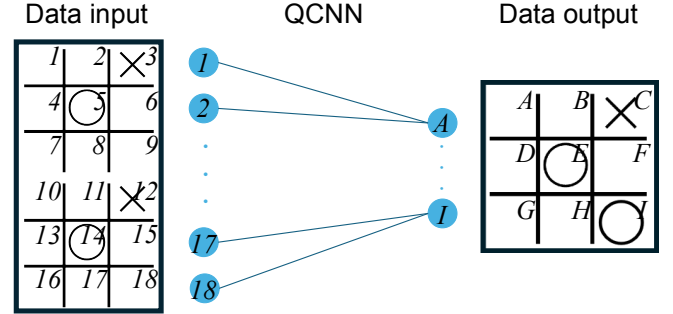


FIGURE 8. Data flow in the quantum convolutional neural network (QCNN) engine. The board is encoded as a 9-dimensional vector and duplicated to match the 18-qubit input requirement. After passing through the QCNN layer, the output is mapped to nine values representing board cells. The move with the highest score is selected.

C. HYBRID NEURAL NETWORKS (CQCNN)

The hybrid engine (CQCNN) combines classical and quantum neural network components. The input and output layers are implemented using classical convolutional neural networks (CNNs), while the hidden layer consists of a quantum neural network, either a QNN or a QCNN, depending on the configuration (Fig. 9).

To accommodate quantum processing, the input board state is first converted into a 9-dimensional vector using the same encoding as in the classical models (O: +1, X: -1, empty: 0). This vector is then expanded to match the number of qubits used in the quantum layer (7 or 18 qubits, depending on the setup), and embedded into quantum states using one of the four encoding methods: HEE, TPE, ZFeatureMap, or ZZFeatureMap.

Two types of quantum neural network layers are used:

- **QNN:** A generic quantum circuit without convolutional structure.

- **QCNN**: A structured ansatz with convolution and pooling layers, as shown in Fig. 16.

The quantum layer is followed by measurement in the Z-basis. We consider two measurement strategies:

- **Estimator**: Returns the expectation value of observables.
- **Sampler**: Returns the frequency distribution of measurement outcomes, treated as probabilities.

In the QNN-based configurations, two types of parameterized quantum circuits (ansatz) are used: `EfficientSU2` and `RealAmplitudes`, both provided by Qiskit. In contrast, the QCNN-based models use a fixed QCNN ansatz with a convolution–pooling structure, and do not incorporate these two ansatz types.

The measured values are passed to the output CNN layer, which produces a 9-dimensional vector corresponding to the tic-tac-toe board cells. The cell with the highest value is selected as the next move. Training is performed using the same reinforcement learning scheme and optimization methods as described in the previous sections.

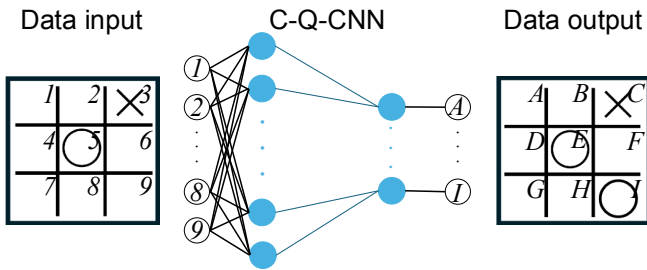


FIGURE 9. Data flow in the hybrid classical–quantum–classical neural network (CQCNN) engine. Encoded board data is processed through an input CNN layer, followed by a quantum layer (QNN or QCNN), and a final output CNN layer. The resulting nine output values are used to determine the next move.

The number of shots in the measurement is set to 1000. We output from the quantum layer in 2 different methods, Estimator and Sampler. Estimator outputs the expected value for each observable after the measurement. Sampler outputs the quasi-probabilities after the measurement. In these engines we used, qubits are measured in the Z basis.

IV. EVALUATION OF ENGINES

In this section, we evaluate 46 game engine configurations across classical, quantum, and hybrid neural network architectures. Each engine is trained using the reinforcement learning method described in Section II and evaluated using Elo ratings obtained through self-play against a random policy.

A. OVERVIEW OF EVALUATION SETTINGS

We present a summary of engine types, training settings, and the resulting performance metrics.

The 46 engines are categorized as follows:

- 1) **Classical CNN engines**: 2 variants with different network depths (see Table 1 (a)).

- 2) **QCNN engines**: 4 configurations using different embedding methods (Table 1 (b)).
- 3) **Hybrid CQCNN engines (QNN layer)**: 32 variants (2 measurement methods \times 2 qubit counts \times 8 configurations).
- 4) **Hybrid CQCNN engines (QCNN layer)**: 8 variants with 2 qubit settings and 4 embedding types.

TABLE 1. NN Architectures: (a) CNN: Stronger has 3 layers, Weaker has 2, both using 3×3 kernels. Stronger also has larger fully connected layers. (b) QCNN: A simple architecture with a single QCNN layer, where the input board is duplicated to match its inputs. (c) CQCNN: $N = 7$ or 18 for QNN, 10 or 18 for QCNN. CQCNNs with a QNN hidden layer support Sampler and Estimator outputs, while those with a QCNN hidden layer support only Estimator.

(a) CNN Architectures			
Engine	Layer	Kernel Size	Output Size
Stronger	Conv	3×3	$1 \times 1 \times 64$
	Flatten	-	64
	Fully Connected 1	-	128
	Fully Connected 2	-	9
Weaker	Conv	3×3	$1 \times 1 \times 16$
	Flatten	-	16
	Fully Connected	-	9
(b) QCNN Architectures			
	Layer		Output Size
	Flatten		18
	QCNN		9
(c) CQCNN Architectures			
Output method	Layer		Output Size
Sampler	Fully Connected 1		N
	QNN		2^N
	Fully Connected 2		9
Estimator	Fully Connected 1		N
	QNN/QCNN		N
	Fully Connected 2		9

These engines used the Tanh function as the activation function before outputting. All engines were trained for 250 games and evaluated over 10,000 games. Elo ratings were updated every 100 games using $K = 1$ in Eq. (3).

B. PERFORMANCE COMPARISON BY ARCHITECTURE

Table 2 summarizes Elo ratings of representative models. Classical CNN engines achieved the highest rating of 1891, followed by hybrid CQCNN models with QNNs, then those with QCNNs, and finally standalone QCNN engines.

Models using 18 qubits tended to perform worse than those with fewer qubits, likely due to overparameterization relative to the simplicity of tic-tac-toe. The two CNN engines listed give a rough idea of the position of the CQCNN engines.

C. DEMONSTRATION USING IBM QUANTUM HARDWARE

To validate the feasibility of executing the proposed engine on real quantum hardware, we deployed the trained model on the `ibm_kawasaki` backend via the IBM Quantum platform. Two matches were conducted: one where the quantum engine played first and another where it played second.

As shown in Fig. 10 and Fig. 11, the quantum engine demonstrated an ability to align symbols strategically, but failed to defend effectively in the endgame. This indicates that

TABLE 2. Main engines and the Elo rating: Roughly speaking, the engines are divided into the following order from highest rating to lowest: classical, CQCNN with QNN as the hidden layer, CQCNN with QCNN as the hidden layer, and QCNN. Even QCNN, which has the lowest rating among the engines, has a difference of 1609, or nearly 100, which gives it a win rate of about 65%, referring to Fig. 5.

type	model	rating
classical neural networks	stronger	1891
Sampler 7 qubit	HEE & EfficientSU2	1809
Estimator 7 qubit	HEE & RealAmplitudes	1776
Estimator 18 qubit	TPE & RealAmplitudes	1762
Sampler 18 qubit	TPE & EfficientSU2	1752
cqcqcn 10 qubit	ZFeatureMap	1751
cqcqcn 18 qubit	HEE	1713
classical neural network	weaker	1712
qcnn 18 qubit	ZZFeatureMap	1609
random policy	-	1500

while the model captures some tactical features, further training or task-specific tuning may be necessary for robustness.

These results demonstrate that even with current hardware constraints, quantum-based game engines can be used in real-world interactive settings.

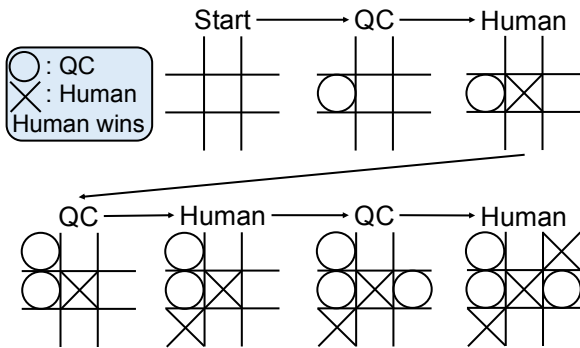


FIGURE 10. Quantum computer vs Human: The quantum computer was first and a human was second. Looking at the quantum computer's moves, the first move was not so bad, but in the middle of the game it could be seen that it was trying to align vertically. However, the game was over without defence when the human tried to align diagonally in the endgame.

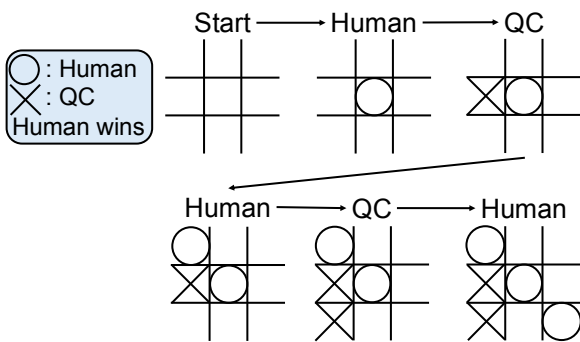


FIGURE 11. Human vs Quantum computer: A human was first and the quantum computer was second. The quantum computer's move showed that it was trying to align vertically, but it did not interfere with the human move and the game was over.

V. THE OVERHEAD OF ENGINES THROUGH QI MODEL

Building upon the client-server quantum machine learning framework described in Section II-D, we evaluate the performance degradation caused by noisy quantum channels in two representative models (Model 1 and Model 2).

A. TOY MODEL SETTINGS

We consider two models of quantum communication channels, depending on the quantum resources available on the client side.

- **Model 1:** The client can embed quantum states and perform measurements.
- **Model 2:** The client cannot measure the quantum states after server-side computation; instead, the server performs the measurement and returns the result to the client.

A schematic diagram of these quantum communication models is shown in Fig. 12. In both models, only noise in the quantum communication channel is considered.

We employ a 7-qubit CQCNN using Sampler, with different Embedding and Ansatz. Noise is introduced by inserting a rotation gate between the quantum circuits of the engine, with its parameters randomized to pseudo-realize the noise effect.

The noise strength depends on the quantum communication distance and is modeled by the following function:

$$\sigma(d) = 10^{\frac{\alpha}{10}d} - 1 \quad (4)$$

where $\sigma(d)$ represents the standard deviation of the noise strength, and $\alpha = 0.2$ dB/km. Gaussian noise is applied to each parameter with a standard deviation of $\sigma(d)$.

The evaluation consists of two experiments:

- 1) **Fixed Distance Experiment:** We assess the engine performance under three noise patterns, with the distance set to 15 km.
 - Pattern A: Noiseless during training and evaluation.
 - Pattern B: Noiseless during training, but noised during evaluation.
 - Pattern C: Noised during both training and evaluation.
- 2) **Distance-Dependent Experiment:** We vary the communication distance from 0 km to 15 km in increments of 3 km and evaluate the engine under Pattern B.

B. THE EFFECT OF NOISY QUANTUM COMMUNICATION

Table. 3 presents the results for different noise models and engines. Fig. 13 and Fig. 14 illustrate the rating transitions of the engines listed in the first row of Table. 3.

The Elo ratings of all engines in Table. 3 follow the order Pattern A, Pattern B and Pattern C, indicating that noise negatively impacts performance. However, the extent of the rating drop varies depending on the engine.

For instance, in Model 1, the engine using HEE and EfficientSU2 shows a significant gap between Pattern

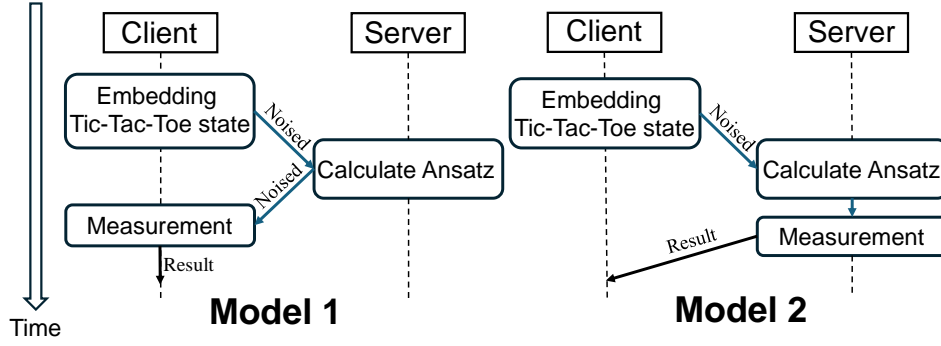


FIGURE 12. Quantum communication model: In Model 1, the client embeds classical data into a qubit, passes it to the server, which calculates the ansatz and then returns it to the client. The client measures the qubit and obtains an output. In Model 2, the client embeds classical data into qubits, passes them to the server, calculates the ansatz, and then makes a measurement. The measurement results are returned to the client and an output is obtained.

TABLE 3. The result of using different noise models and engines: The table features 3 different engines in each model.

engine	model	train	evaluate	rating
Sampler HEE EfficientSU2	1	noiseless	noiseless	1728
		noiseless	noised	1630
		noised	noised	1619
	2	noiseless	noiseless	1692
		noiseless	noised	1621
		noised	noised	1537
Sampler ZFeatureMap RealAmplitudes	1	noiseless	noiseless	1685
		noiseless	noised	1684
		noised	noised	1573
	2	noiseless	noiseless	1711
		noiseless	noised	1663
		noised	noised	1554
Sampler ZZFeatureMap RealAmplitudes	1	noiseless	noiseless	1731
		noiseless	noised	1675
		noised	noised	1431
	2	noiseless	noiseless	1677
		noiseless	noised	1651
		noised	noised	1548

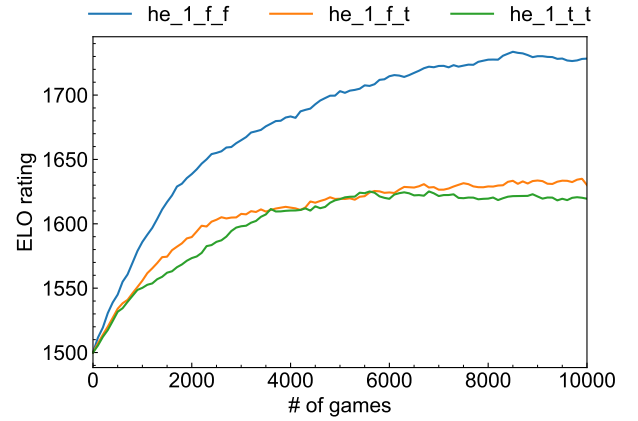


FIGURE 13. Transition of ratings when evaluating engines using HEE and EfficientSU2: **he_1** represents Model 1 using HEE and EfficientSU2. **he_1_ff** is the Pattern A, **he_1_ft** is the Pattern B, and **he_1_tt** is the Pattern C.

A and the others, whereas Patterns B and C yield similar ratings. In contrast, the engine using ZFeatureMap and RealAmplitudes in Model 1 exhibits similar ratings for Patterns A and B, but a significant drop in Pattern C. These differences suggest that the robustness to noise depends on the choice of embedding and ansatz.

Fig. 13 and Fig. 14 show the progression of the rating in every 100 games. In both figures, Pattern A exhibits a steady increase in ratings, while Patterns B and C show slower growth due to the effects of noise.

Fig. 15 illustrates the rating transition as a function of distance. As shown in the figure, there is a sharp drop in the ratings between 0 and 3 km, followed by a more gradual decline as the distance increases. This suggests that the initial increase in noise significantly impacts accuracy, but beyond a certain distance, the degradation stabilizes.

VI. CONCLUSION

In this study, we built game engines using classical, quantum, and classical-quantum hybrid neural networks and compared

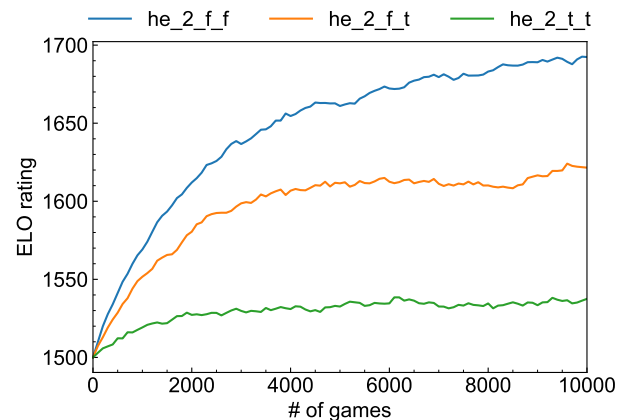


FIGURE 14. Transition of ratings when evaluating engines using HEE and EfficientSU2: **he_2** represents Model 2 using HEE and EfficientSU2. **he_2_ff** is the Pattern A, **he_2_ft** is the Pattern B, and **he_2_tt** is the Pattern C.

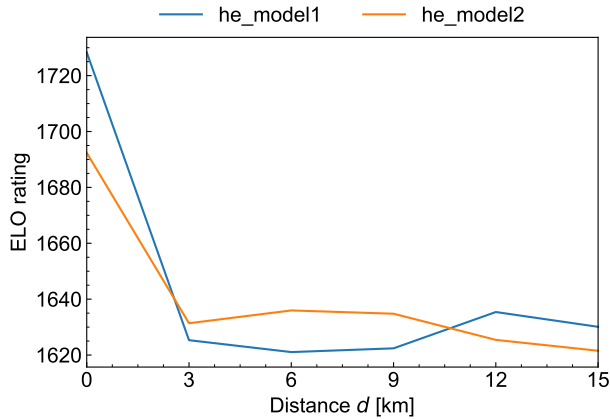


FIGURE 15. Transition of ratings per distance: he_model1 represents Model 1 using HEE and EfficientSU2, and he_model2 is Model 2 using HEE and EfficientSU2.

their performances. By comparing the performance of each engine in terms of ratings, we can determine the relative strength of the engines. In the same way that the development of computers and algorithms has led to the development of classical game engines such as chess, the development of quantum computers and quantum algorithms is expected to contribute to the development of quantum game engines as they are developed.

Although it was difficult for the quantum computer to outperform classical methods due to the game of tic-tac-toe in this study, the objective of comparing the different engines through the rating was achieved. We also modeled a simple noisy communication channel, which can be used not only for the game solver task but also as a guide for developing various quantum network applications, and verified the amount of overhead observed. This is a necessary indicator not only for simple applications but also for the development of hidden applications. It will be a stepping stone to develop use cases of quantum network applications that are better than classical ones, while taking noise into account.

APPENDIX A QUANTUM ENGINE CONFIGURATIONS

A. QUANTUM CIRCUITS

Fig. 16 shows Embedding and Ansatz used in this paper.

ZFeatureMap, ZZFeatureMap, RealAmplitudes and EfficientSU2 are referred to the qiskit library. HEE and TPE are referred to the circuit for embedding in [23], and QCNN is referred to the circuit in [24] and Qiskit machine learning tutorial.

B. ENGINE PROPERTIES AND RATING

Table 4 lists the 46 engines mentioned in Sec. IV and their ratings and other detailed information.

ACKNOWLEDGMENT

SK, HK, SN, and TS are supported by JST Moonshot R&D Grant Number JPMJMS226C. SK and TS are also supported by JST COI-NEXT Grant Number JPMJPF2221. SN is also supported by JSPS KAKENHI Grant Number JP2KJ1436. TS is also supported by MEXT KAKENHI Grant Number 22K1978.

REFERENCES

- [1] Peter W. Shor. Polynomial-time algorithms for prime factorization and discrete logarithms on a quantum computer. *SIAM Journal on Computing*, 26(5):1484–1509, October 1997.
- [2] Lov K. Grover. A fast quantum mechanical algorithm for database search, 1996.
- [3] Amara Katabarwa, Katerina Gratsea, Athena Caesura, and Peter D. Johnson. Early fault-tolerant quantum computing. *PRX Quantum*, 5(2), June 2024.
- [4] Alexis Morvan, B Villalonga, X Mi, S Mandra, A Bengtsson, PV Klimov, Z.Chen, S Hong, C Erickson, IK Drozdov, et al. Phase transitions in random circuit sampling. *Nature*, 634(8033):328–333, 2024.
- [5] Youngseok Kim, Andrew Eddins, Sajant Anand, Ken Xuan Wei, Ewout Van Den Berg, Sami Rosenblatt, Hasan Nayfeh, Yantao Wu, Michael Zaletel, Kristan Temme, et al. Evidence for the utility of quantum computing before fault tolerance. *Nature*, 618(7965):500–505, 2023.
- [6] David Silver, Thomas Hubert, Julian Schrittwieser, Ioannis Antonoglou, Matthew Lai, Arthur Guez, Marc Lanctot, Laurent Sifre, Dharrshan Kumaran, Thore Graepel, Timothy Lillicrap, Karen Simonyan, and Demis Hassabis. A general reinforcement learning algorithm that masters chess, shogi, and go through self-play. *Science*, 362(6419):1140–1144, 2018.
- [7] IBM. Ibm quantum challenge 2020, 2020. <https://github.com/qiskit-community/IBMQuantumChallenge2020>.
- [8] Christopher JCH Watkins and Peter Dayan. Q-learning. *Machine learning*, 8:279–292, 1992.
- [9] Jacob Biamonte, Peter Wittek, Nicola Pancotti, Patrick Rebentrost, Nathan Wiebe, and Seth Lloyd. Quantum machine learning. *Nature*, 549(7671):195–202, 2017.
- [10] Maria Schuld, Ilya Sinayskiy, and Francesco Petruccione. An introduction to quantum machine learning. *Contemporary Physics*, 56(2):172–185, 2015.
- [11] Jordanis Kerenidis and Anupam Prakash. Quantum gradient descent for linear systems and least squares. *Physical Review A*, 101(2):022316, 2020.
- [12] James Stokes, Josh Izaac, Nathan Killoran, and Giuseppe Carleo. Quantum natural gradient. *Quantum*, 4:269, 2020.
- [13] Iris Cong, Soonwon Choi, and Mikhail D Lukin. Quantum convolutional neural networks. *Nature Physics*, 15(12):1273–1278, 2019.
- [14] Arthur Pesah, Marco Cerezo, Samson Wang, Tyler Volkoff, Andrew T Sornborger, and Patrick J Coles. Absence of barren plateaus in quantum convolutional neural networks. *Physical Review X*, 11(4):041011, 2021.
- [15] Arpad E. Elo and Sam Sloan. *The rating of chessplayers : past and present*. Ishi Press International, 2008.
- [16] Paul CH Albers and Han de Vries. Elo-rating as a tool in the sequential estimation of dominance strengths, 2001.
- [17] Lars Magnus Hvattum and Halvard Arntzen. Using elo ratings for match result prediction in association football. *International Journal of Forecasting*, 26(3):460–470, 2010. Sports Forecasting.
- [18] Arnaldo Rafael Camara Araujo, Ogochuchi Daniel Okey, Muhammad Saadi, Pablo Adasme, Renata Lopes Rosa, and Demóstenes Zegarra Rodríguez. Quantum-assisted federated intelligent diagnosis algorithm with variational training supported by 5g networks. *Scientific Reports*, 14(1):26333, 2024.
- [19] Yanqi Song, Yusen Wu, Shengyao Wu, Dandan Li, Qiaoyan Wen, Sujuan Qin, and Fei Gao. A quantum federated learning framework for classical clients. *Science China Physics, Mechanics & Astronomy*, 67(5):250311, 2024.
- [20] Ali Javadi-Abhari, Matthew Treinish, Kevin Krsulich, Christopher J. Wood, Jake Lishman, Julien Gacon, Simon Martiel, Paul D. Nation, Lev S. Bishop, Andrew W. Cross, Blake R. Johnson, and Jay M. Gambetta. Quantum computing with Qiskit, 2024.
- [21] Peter J Huber. Robust estimation of a location parameter. In *Breakthroughs in statistics: Methodology and distribution*, pages 492–518. Springer, 1992.

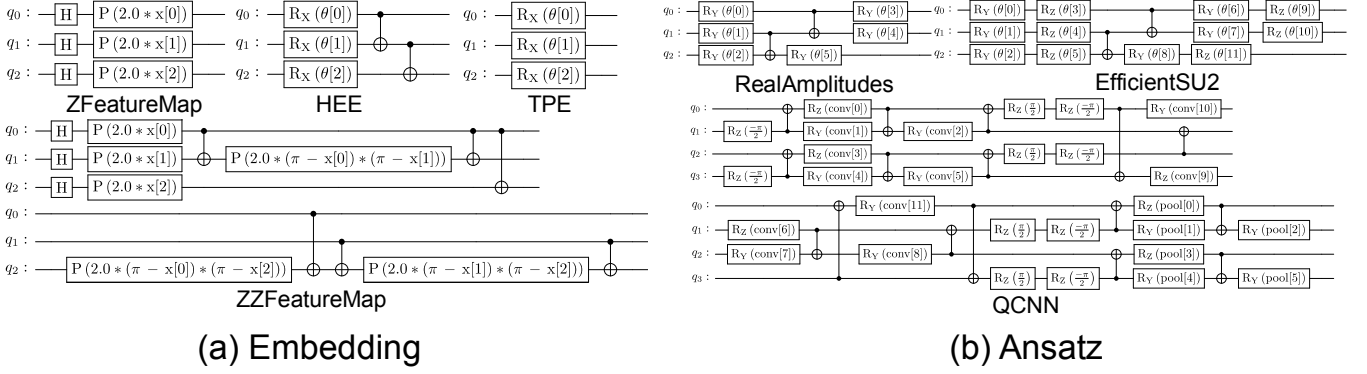


FIGURE 16. Embedding and Ansatz used in engines: (a) Embedding is a quantum circuit for embedding certain classical data into qubits. ZFeatureMap and ZZFeatureMap were built using the qiskit library, while HEE and TPE were constructed by referring to the circuit for embedding in [23]. (b) Ansatz is a circuit for processing data embedded in qubits using weight parameters. RealAmplitudes and EfficientSU2 were built using the qiskit library. QCNN referred to the circuit in [24] and Qiskit machine learning tutorial.

- [22] Diederik P Kingma and Jimmy Ba. Adam: A method for stochastic optimization. *arXiv preprint arXiv:1412.6980*, 2014.
- [23] Supanut Thanasilp, Samson Wang, Nhat Anh Nghiem, Patrick Coles, and Marco Cerezo. Subtleties in the trainability of quantum machine learning models. *Quantum Machine Intelligence*, 5(1), May 2023.
- [24] Farrokh Vatan and Colin Williams. Optimal quantum circuits for general two-qubit gates. *Physical Review A*, 69(3), March 2004.

...

TABLE 4. Properties and Elo ratings of 46 engines: This table is divided into eight rows, which can be classified as follows: (a) the first row, (b) rows 2-5, (c) rows 6-7, and (d) the eighth row. (a) is 2 types of engines using only CNN. (b) is 32 types of engines using CQCNN with QNN. (c) is 8 types of engines using CQCNN with QCNN. (d) is 4 types of engines using only QCNN.

type	model	rating	classical params	quantum params	total params	CX gates	depth
classical neural network	stronger	1891	10057	-	10057	-	-
	weaker	1712	297	-	297	-	-
sampler 7 qubit	ZFeatureMap+RealAmplitudes	1705	1231	21	1252	6	10
	ZZFeatureMap+RealAmplitudes	1625				48	43
	HEE+RealAmplitudes	1735				12	15
	TPE+RealAmplitudes	1686				6	9
	ZFeatureMap+EfficientSU2	1716		35	1266	6	12
	ZZFeatureMap+EfficientSU2	1568				48	45
	HEE+EfficientSU2	1809				12	17
	TPE+EfficientSU2	1779				6	11
sampler 18 qubit	ZFeatureMap+RealAmplitudes	1737	2359485	54	2359539	17	21
	ZZFeatureMap+RealAmplitudes	1550				323	120
	HEE+RealAmplitudes	1535				34	37
	TPE+RealAmplitudes	1693				17	20
	ZFeatureMap+EfficientSU2	1662		90	2359575	17	23
	ZZFeatureMap+EfficientSU2	1476				323	122
	HEE+EfficientSU2	1708				34	39
	TPE+EfficientSU2	1752				17	22
estimator 7 qubit	ZFeatureMap+RealAmplitudes	1725	142	21	163	6	10
	ZZFeatureMap+RealAmplitudes	1491				48	43
	HEE+RealAmplitudes	1776				12	15
	TPE+RealAmplitudes	1686				6	9
	ZFeatureMap+EfficientSU2	1720		35	177	6	12
	ZZFeatureMap+EfficientSU2	1452				48	45
	HEE+EfficientSU2	1683				12	17
	TPE+EfficientSU2	1625				6	11
estimator 18 qubit	ZFeatureMap+RealAmplitudes	1700	351	54	405	17	21
	ZZFeatureMap+RealAmplitudes	1553				323	120
	HEE+RealAmplitudes	1742				34	37
	TPE+RealAmplitudes	1762				17	20
	ZFeatureMap+EfficientSU2	1633		90	441	17	23
	ZZFeatureMap+EfficientSU2	1564				323	122
	HEE+EfficientSU2	1753				34	39
	TPE+EfficientSU2	1729				17	22
cqccqnn 10 qubit	ZFeatureMap	1751	154	55	209	40	17
	ZZFeatureMap	1299				130	68
	HEE	1602				49	25
	TPE	1645				40	16
cqccqnn 18 qubit	ZFeatureMap	1698	270	99	369	72	17
	ZZFeatureMap	1578				378	116
	HEE	1713				89	33
	TPE	1398				72	16
qcnn 18 qubit	ZFeatureMap	1585	-	99	99	72	17
	ZZFeatureMap	1609	-			378	116
	HEE	1493	-			89	33
	TPE	1339	-			72	16